3 New Experimetal Facilities and Apparatus

3-1 A High-Resolution ARPES Spectrometer Combined with a Combinatorial Laser MBE Thin Film Growth System

We have constructed a high-resolution angle-resolved photoemission (ARPES) spectrometer combined with a combinatorial laser molecular-beam epitaxy (laser MBE) thin film growth system in order to investigate the electronic structure of transition metal oxide (TMO) thin films. The system is installed at either the high-resolution vacuum-ultraviolet beamline BL-1C or the soft-X-ray undulator beamline BL-2C as an end-station. In this system (Fig. 1), a total energy resolution of 6.3 meV and a momentum (*i.e.* angular) resolution of 0.02 Å^{-1} (0.2°) were obtained at a photon energy of 40 eV. Laser MBE-grown thin film samples can be transferred quickly into the photoemission chamber without breaking ultrahigh vacuum. Laser MBE is one of the best methods for growing thin films of many different transition metal oxides and achieving the well-ordered surfaces which are essential for ARPES measurements. The capabilities of the system and the importance of the *in situ* sample transfer between the ARPES and the laser MBE systems are demonstrated with a study of the band structure of $La_{0.6}Sr_{0.4}MnO_3$ thin films.

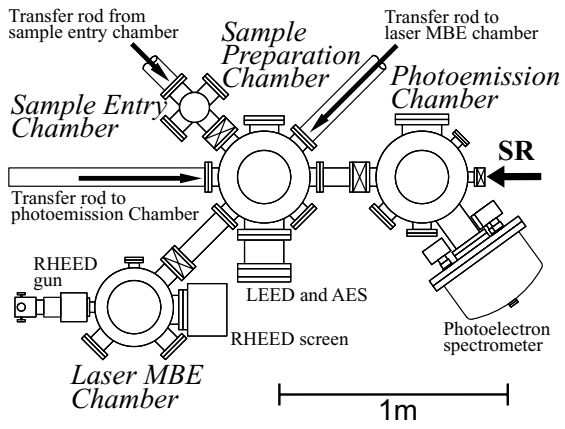

Figure 1
A schematic diagram of an *in situ* ARPES - laser MBE system.

The growth and ARPES measurement of $La_{0.6}Sr_{0.4}MnO_3$ (LSMO) thin films using the *in situ* ARPES-laser MBE system were performed at BL-1C. LSMO thin films with a thickness of about 400 Å were deposited on TiO_2-terminated $SrTiO_3$(001) (STO) substrates at a substrate temperature of 950°C. Epitaxial growth of LSMO thin films was confirmed by the observation of clear RHEED oscillations. The films were then moved into the photoemission chamber. The ARPES spectra were taken at 150 K using a GAMMADATA SCIENTA SES-100 electron-energy analyzer operating in angle-resolved mode. The surface morphology of the measured films was analyzed by ex situ atomic force microscopy in air and an atomically flat step-and-terrace structure was observed.

Figure 2(b) shows ARPES spectra of an LSMO thin film recorded at various photon energies between 30 and 70 eV at normal emission. We find that the ARPES spectra exhibit considerable and systematic changes as a function of photon energy; highly dispersive features with

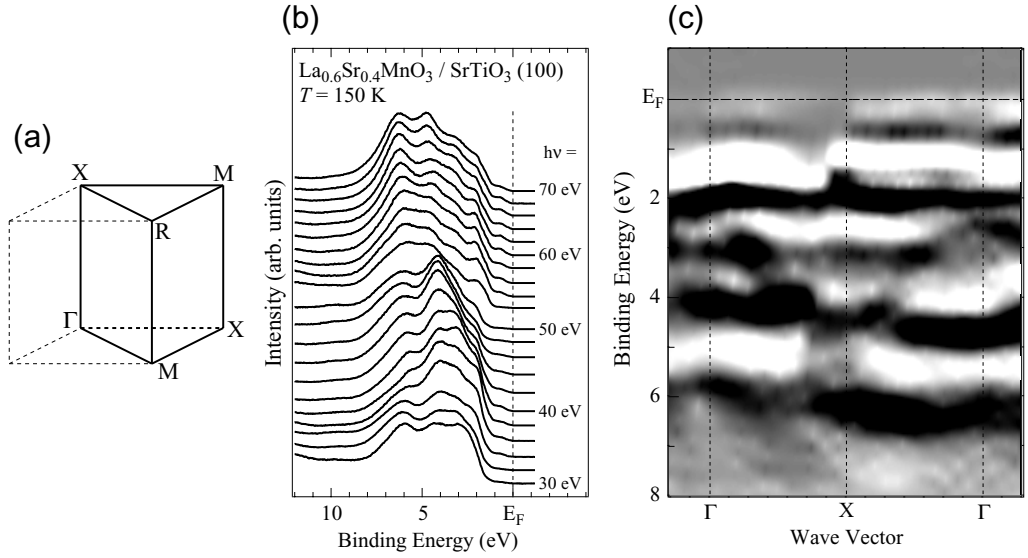

Figure 2
(a) Brillouin zone of cubic perovskite structure. (b) ARPES of a LSMO epitaxial thin film grown by laser MBE. (c) Experimental band structure of the LSMO thin film. Dark areas correspond to the energy bands.

a band-width of about 2 eV exist in the energy range of 2-5 eV. Figure 2(c) shows the experimental band structure of LSMO thin films along the Γ–X direction in the Brillouin zone of the cubic perovskite structure derived from the present normal emission ARPES measurement. The dark areas of the plot correspond to the energy bands. As expected from the ARPES spectra, several dispersive bands are clearly observed, demonstrating that we have succeeded in the ARPES measurement of LSMO thin films. These results indicate that the *in situ* ARPES measurement combined with laser MBE is a unique and powerful experimental technique for determining the electronic band structures of oxides even when there are no cleavable planes. We believe that *in situ* ARPES studies on TMO thin films with well-ordered surfaces can provide a wealth of information on the electronic structure of oxides, and is a key technique for understanding their remarkable physical properties.

3-2 Performance of the Photon Microbeam Irradiation System for Radiobiology

Risk evaluation of low dose radiation is now becoming of great concern, not only to radiobiologists but also to all the members of modern society. The biological effects of radiation are initiated by the energy of the radiation. Since the energy is deposited by charged particles, the lowest amount of energy, or dose, will be given to the cell when only one track has passed through. In the case of an α particle, this minimum dose to the cell is of the order of 0.1 Gy, and 1 mGy in the case of an electron. In cell populations irradiated with doses lower than these values, the number of cells which have not accepted any traversal of particles becomes larger than the number of cells which have accepted a traversal. In order to study the radiation effects of hit-cells in a majority non-hit cell population, we have developed a microbeam irradiation system using monochromatic soft X-rays by which we can irradiate each cell individually. The performance of the system, installed at BL-27B, is summarized below.

X-ray energy and beam size

In order to keep the cell in a good physiological condition even during irradiation, we have developed a specially designed dish, the bottom of which is composed of a thin (1.5 μm) film. Cells are grown on this dish before irradiation, and irradiated from below. To deflect the horizontal SR beam upwards by 90°, we use a Si(311) crystal. The energy of the X-rays is determined to be 5.35 keV. A monochromatic X-ray microbeam deposits this energy in a cylindrical volume of X-ray beam path in the sample after giving its energy to secondary photoelectrons. Thermalization length of a 5-keV photoelectron is known to be 0.78 μm, so the energy due to the radiation is not scattered outside of this beam area. Accordingly, we have proposed a beam size of a few μm, small enough to aim at cell nuclei which contain DNA, and that we can expect the X-ray energy to be distributed around the designated area in the sample.

We have already succeeded in generating a microbeam of 2 μm by using a K-B mirror system. Due to the complexity of setting up the mirror system, however, we use a slit system to obtain the microbeam, and the beam size available is 5 μm^2 or larger (adjustable). The dose rate is about 6 Gy/min, independent of the beam size.

Cell recognition and positioning

Cells to be irradiated are stained with appropriate fluorescent dyes, and the fluorescence image is captured by a CCD camera and analyzed with appropriate software to recognize cells or nuclei within cells. The positions of these targets are calculated and memorized for the positioning of the irradiation target.

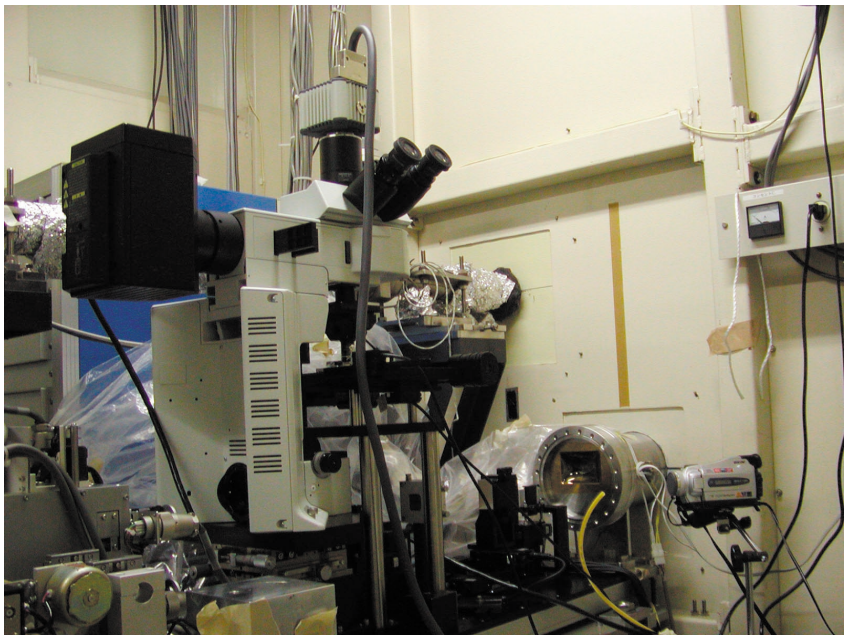

Figure 3
Photograph of the developed microbeam irradiation system setup at BL-27B.

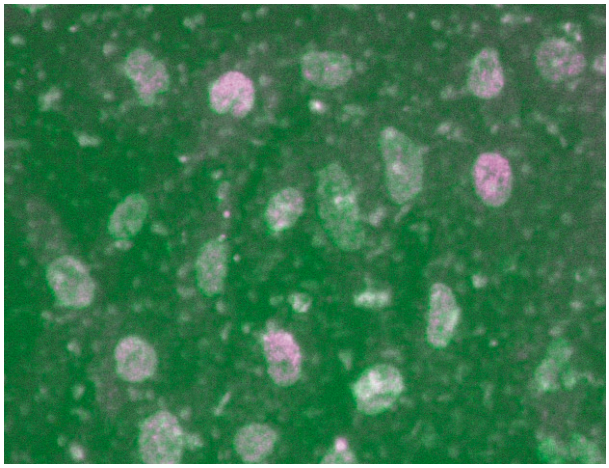

Figure 4
Fluorescent image of microbeam-irradiated cells. Only three cells, located in a triangle, are identified as immuno-stained with the antibody for γ-H2AX, specifically associated with the double strand breaking of DNA.

Accuracy/reproducibility of the target positioning

The motorized precision stage we use is equipped with linear encoders of 0.5 μm accuracy. However, the overall reproducibility of the system is determined also by the distortion of the components in the imaging system, such as optical distortion in the image field by the microscope and positional deviation of pixels in the CCD camera. In order to check the accuracy of the obtained coordinates of the target, we have tested the accuracy/reproducibility of the targeting using fluorescent microspheres (5 μm in diameter)-immobilized dish. We follow the procedure to identify the cells and during the process of irradiation the positional deviation from the center of the beam position of each sphere is measured. The averaged value of the deviation was 1.5 μm, which was considered small enough to be able to aim at cell nuclei.

We have also tested whether the sample cells could be found and identified when the sample dish was returned to the system after various post-irradiation treatments. It was found that irradiated targets can easily be identified on the sample dish once-detached after irradiation. A photograph of the whole system is shown in Fig. 3.

System control software

We have developed software written with Visual Basic, calling *ImageProPlus* as a subroutine. This software can control all of the processes including image-capturing, image analysis, stage movement and X-ray irradiation, although some improvement is underway.

Recently, we have succeeded in observing the γ-H2AX immuno-staining of irradiated cell nuclei, used to identify double strand breaks in DNA, as shown in Fig. 4. The region mode, in which the designated area is scanned to search for the target following which the identified target is automatically irradiated with the desired X-ray dose, will be available in autumn of 2003.

3-3 Completion of Slow Positron Beamline at a New Site

Construction of a new slow positron beamline with a time of flight positronium spectrometer (Fig. 5) has been completed at a site next to the 40-MeV Test Linac which is dedicated to producing slow positrons. All of the required radiation safety examinations were successfully carried out, and some test data have been obtained (Fig. 6) prior to public use.

The characteristics of the slow positron beam are as follows:

Beam size: 10 mm in diameter.
Energy: a few eV-9 keV.
Pulse width: 22 ns.
Duty cycle: 50 Hz.
Number of positrons: 5×10^6/s.

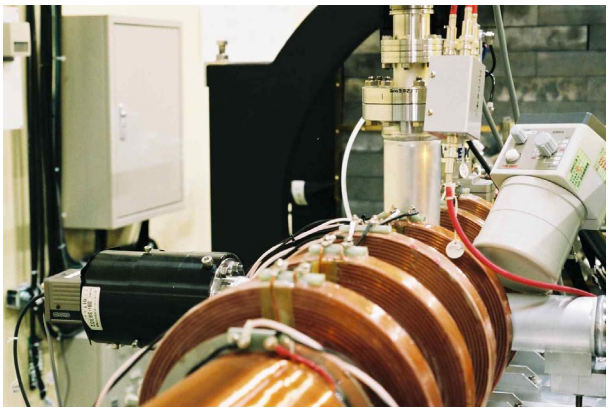

Figure 5
Side view of of the time of flight positronium (Ps) spectrometer.

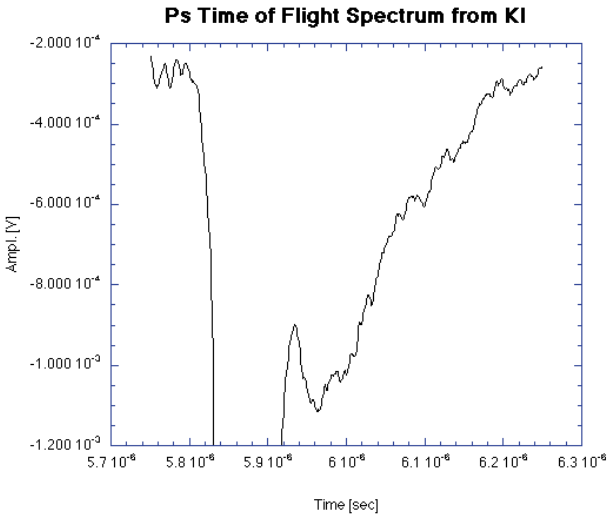

Figure 6
Typical time of flight spectrum of Ps emitted from KI. The position at 5870 ns represents 511 keV annhilation radiation and the peak at 5970 ns represents Ps emitted from KI at room temperature.